

TITLE PAGE

Title:

Voltage-gated Sodium Channels Regulating Action Potential Generation in Itch-, Nociceptive-, and Low-Threshold Mechanosensitive Cutaneous C-fibers

Authors:

Danica Jurcakova

Fei Ru

Marian Kollarik

Hui Sun

Jeffrey Krajewski

Bradley J. Udem

Affiliation:

Department of Medicine, Johns Hopkins University School of Medicine, Baltimore, MD 21224, USA

(D.J., F.R., M.K., H.S., B.J.U)

Comenius University in Bratislava, Jessenius Faculty of Medicine in Martin (JFM CU), Biomedical

Center Martin JFM CU and Department of Pathophysiology JFM CU, 036 01 Martin, Slovakia (D.J.,

M.K)

Lilly Research Laboratories, Indianapolis, IN 46225, USA (J.K.)

RUNNING TITLE PAGE

Running title: Na_v1 channels in itch and pain C-fibers

Corresponding author:

Bradley J. Udem

Address: Department of Medicine, Johns Hopkins University School of Medicine, 5501 Hopkins

Bayview Circle, Baltimore, MD 21224, USA

tel.: 410-550-2160

email: bundem@jhmi.edu

Number of text pages: 23

Number of tables: 2

Number of figures: 6

Number of references: 34

Number of words in Abstract: 233

Number of words in Introduction: 591

Number of words in Discussion: 1500

List of non-standard abbreviations

α,β-meATP alpha,beta-methylene ATP

CQ chloroquine

C-HTMs high-threshold mechanosensitive C-fibers

C-LTMs low-threshold mechanosensitive C-fibers

HA histamine

Na_vs voltage-gated sodium channels

TTX tetrodotoxin

5-HT 5-hydroxytryptamine (serotonin)

ABSTRACT

We evaluated the effect of voltage-gated sodium channel 1 (Na_v1) blockers in three non-overlapping C-fiber subtypes in the mouse skin: namely, chloroquine (CQ)-sensitive C-fibers with high mechanical thresholds – ostensibly *itch C-fibers*; secondly, CQ-insensitive, capsaicin-sensitive C-fibers with high mechanical thresholds – ostensibly *nociceptors*; and CQ and capsaicin-insensitive C-fibers with very low mechanical threshold – *C-LTMs*. Na_v1 blocking drugs were applied to the nerve terminal receptive fields using an innervated isolated dorsal mouse skin-nerve preparation where the drugs are delivered into the skin intra-arterially. We combined these studies with an analysis of the mRNA expression of the α subunits of Na_v1s in individual dorsal root ganglia neurons labeled from the same region of the skin. Our results show that virtually all nociceptors and itch C-fibers expressed the tetrodotoxin (TTX)-resistant channels Na_v1.8 and Na_v1.9. However, TTX applied selectively into the skin abolished the action potential firing in response to mechanical stimulation in 75% of the itch C-fibers, 100% of the nociceptors, and 100% of C-LTMs. Na_v1.7 was the most commonly expressed TTX-sensitive Na_v1 in all three C-fiber subtypes innervating the dorsal skin. Selectively blocking Na_v1.7 abolished responses in about 40% of itch C-fibers, 65% of nociceptors, but only 20% of C-LTMs. Blocking Na_v1.8 alone had no effect on the firing sensitivity of the C-fibers. However, in itch- and nociceptive C-fibers where the activation was not inhibited with a Na_v1.7 blocker, adding the Na_v1.8 blocker silenced action potential discharge.

INTRODUCTION

The majority of electrophysiological studies on cutaneous C-fibers in laboratory animals have been focused on nerve fibers terminating in glabrous and non-glabrous aspect of the hind paw.

Electrophysiological recordings from cutaneous sensory nerves reveal subpopulations of C-fibers based on their stimulus profile. Accordingly, there are C-fibers that are unresponsive to mechanical stimulation, those that respond to mechanical stimuli with low and high threshold, those that respond to heat, cold, chemical, inflammatory mediators or some combination therein (Dubin and Patapoutian, 2010; Kress et al., 1992; Lawson et al., 2008).

We recently developed a skin-nerve preparation ideally suitable for investigating the pharmacology of C-fibers terminating in the skin covering the dorsal thorax. Using this technique we noted that essentially all C-fibers terminating in this region of the skin are mechanically sensitive and the vast majority can be stimulated by capsaicin (and presumably therefore also heat) (Ru et al., 2017). Based on their chemical sensitivity profile, the C-fibers can be further subdivided into presumed itch (scratch evoking) C-fibers and nociceptive C-fibers (Han et al., 2013; Liu et al., 2009; Ru et al., 2017). In this study we further analyzed the mechanical and chemical sensitivity of the C-fiber subtypes innervating the dorsal thorax of the mouse.

Regardless of the stimulus, the information from the C-fiber terminal will not reach the central nervous system without the activation of Na_v1 channels during the generation and conduction of an action potential (AP). Among the nine pore-forming alpha-subunits of Na_v1 channels (namely $\text{Na}_v1.1$ – $\text{Na}_v1.9$) all but $\text{Na}_v1.5$ (cardiac) and $\text{Na}_v1.4$ (striated muscle) are commonly expressed in neurons. Tetrodotoxin (TTX), a frequently used toxin to study Na_v1 function, potently and selectively blocks $\text{Na}_v1.1$, 1.2, 1.3, 1.4, 1.6, and 1.7, but has little effect on $\text{Na}_v1.5$, 1.8, and 1.9. The specific Na_v1 subtypes expressed in a nerve depend on the neuronal phenotype (Lai et al., 2004).

Complicating matters is the observation that the nature of the Na_v1 controlling APs may not be constant along different aspects of the nerve. For example, AP generation at the terminals of C-fibers in the cornea does not require TTX-sensitive Na_v1 channels, but the conduction of the AP along the trigeminal axons toward the cell bodies in the trigeminal ganglion is abolished by TTX (Brock et al.,

1998). Likewise, selectively blocking $\text{Na}_v1.7$ can prevent conduction of APs in vagal afferent A- and C-fibers (Kollarik et al., 2018; Muroi et al., 2011). In contrast, blocking $\text{Na}_v1.7$ (and other TTX-sensitive channels) at the terminals of a subset of vagal C-fibers within the trachea or lungs is without effect on chemical induced initiation of action potentials, where $\text{Na}_v1.8$ appears to play a more important role (Kollarik et al., 2018). The same holds in spinal afferent nerves of mice and non-human primates where conduction of APs in afferent axons close to the peripheral tissue of their innervation are more TTX-resistant than conduction along more central aspects of the nerve (Klein et al., 2017).

Characteristics of the Na_v1 s involved in AP generation has benefited greatly from genetic deletion studies, however this strategy eliminates the Na_v channel from all aspects of the nerve. In the present study, we were interested in determining the Na_v1 subtypes involved in AP formation in C-fiber subtypes specifically within the cutaneous compartment, i.e. that aspect of the nerve that would be effectively influenced by topically applied Na_v blocking drugs. This was carried out by taking advantage of Na_v1 subtype selective blockers, combined with an *ex vivo* skin-nerve preparation that allows for the delivery of drugs directly to the nerve's receptive field in the skin via intra-arterial injections.

MATERIALS AND METHODS

Animals

Animals used in experiments were male mice C57BL/6J, 6-8 week old, weighing 22-27g. The mice were housed with a 12-hour light-dark cycle at air temperature 22°C, with access to water and food *ad libitum*. All experiments were approved by the Johns Hopkins Animal Use and Care Committee.

Retrograde labeling of cutaneous nerve fibers

Mice were anaesthetized with 50mg/kg ketamine, 10mg/kg xylazine dissolved in physiological saline. The hair in dorsal skin (Figure 1) were shaved using an electrical razor. Exposed skin was labeled with retrograde tracer 1,1'-Dioctadecyl-3,3,3',3'-tetramethylindocarbocyanine perchlorate (Dil, 0.1% in 10% dimethylsulfoxide:saline mixture) up to total volume 200µl (applied directly on the skin surface). After 14 days, the dorsal root ganglia from treated mice were dissociated and used for cell picking.

Dorsal root ganglia dissociation

We followed the protocol described in detail previously (Kocmalova et al., 2017; Kwong et al., 2008; Ru et al., 2011; Surdenikova et al., 2012). Briefly, mice dorsal root ganglia (T8-T10) were dissected and dissociated by trituration and enzymatic treatment (2 mg/ml collagenase type 1A; 2 mg/ml dispase II in Ca²⁺-, Mg²⁺-free Hanks' balanced salt solution), plated on poly-d-lysine and laminin-coated coverslips and incubated 2 hours at 37°C. The coverslips were flooded with 2ml of L-15 medium supplemented with 10% fetal bovine serum and used within 8 h (for cell picking) or within 24 hours (for patch clamp recording).

Patch clamp recording

Conventional whole-cell patch clamp technique was employed to record the sodium current (I_{Na}) using an Axopatch 200B amplifier interfaced with Axon Digidata 1550A and driven by pCLAMP 10 software (Molecular Devices, Sunnyvale, CA, USA). Bath solution contained (mM): choline-Cl 126, NaCl 10, CsCl 3, TEA-Cl 5, MgCl₂ 1, CaCl₂ 1, CdCl₂ 0.1, HEPES 10 and glucose 10 with pH adjusted to 7.35 with CsOH. Pipette solution contained (mM): CsF 140, NaCl 10, MgCl₂ 1, CaCl₂ 0.1, EGTA 1.1 and HEPES 10 with pH adjusted to 7.2 with CsOH. Cell capacitance and series resistance were

compensated electronically by ~80% to ensure an adequate voltage control. To record I_{Na} , cells were held at -110 mV and two depolarizing pulses, separated by a 1-sec interval at -60 mV, were applied every 5 seconds to voltages ranging from -90 to +20 mV at an increment of 5 mV. The second pulse was used to record the TTX-resistant I_{Na} . The current was sampled at 50 kHz and filtered at 10 kHz.

Cell picking

Coverslips with dissociated neurons were perfused with PBS and Dil-labeled neurons were identified under fluorescent microscope. Neurons free of debris or attached cells were harvested individually into a glass-pipette by applying negative pressure. The pipette tip containing the cell was broken into a PCR tube containing RNase Inhibitor (1 μ L, RNaseOUT, 2 U L⁻¹; Invitrogen), immediately frozen and stored at -20° C. From every coverslip a sample of the bath solution was collected for no-template experiments (bath control).

Single cell RT-PCR

Single cell RT-PCR was performed as described previously (Brozmanova et al., 2016; Liu et al., 2009). Briefly, samples with harvested cells were defrosted and reverse transcription was performed using Super-ScriptTM III CellsDirect cDNA Synthesis System (Invitrogen) according to the manufacturer's recommendations. A total of 2 μ l of cDNA or negative control was used for PCR, performed with HotStar Taq Polymerase Kit (Qiagen) in a final volume of 20 μ l. Intron-spanning primers (Table 2) were designed based on Pubmed sequences and Primer3 (Rozen and Skaletsky, 2000) and some published previously (Kocmalova et al., 2017). PCR products were visualized in a 1.5% agarose gel containing ethidium—bromide using QuantityOne software (Bio-Rad Laboratories).

Ex vivo DRG nerve-skin preparation

Dorsal root ganglia-spinal nerve-skin preparation has been described in detail recently (Ru et al., 2017), and is pictured in Figure 1. Briefly, right dorsal mouse skin (3x3cm) with the main arterial supply (subscapular artery) was dissected along with a spinal nerves and dorsal root ganglia (most often T9 or T8, occasionally T7 or T10). If present, the vessels other than the subscapular artery were ligated to prevent a rapid exit of chemicals infused into subscapular artery. The skin was pinned dermis side up in a Sylgard-lined Perspex tissue chamber, the DRG ganglion with the nerve was

positioned in adjacent Sylgard-lined recording chamber. The tissue and recording chamber were separately superfused with Krebs solution at a flow rate of 4 ml min⁻¹ (temperature 32–34°C) and 3 ml min⁻¹ (36–37°C), respectively. Krebs solution contained indomethacin (3μM) to overcome undesired C-fiber sensitization due to prostanoid release resulting from mechanical probing the skin over time (Emery et al., 2016).

Extracellular recording of DRG fibers in the skin

The method for the extracellular recording from the dorsal root neurons projecting to the skin has been described in detail in Ru et al. (2017). The aluminosilicate glass electrode filled with 3M NaCl was manipulated into the dorsal root ganglia in the recording chamber where a return electrode of silver-silver chloride wire and an earthed silver-silver chloride pellet were situated. The recording signal was amplified (Microelectrode AC amplifier 1800, A-M Systems) and filtered (low cut off, 0.3 kHz; high cut off, 1 kHz) and the resultant activity was displayed on an oscilloscope (TDS 3054B, Tektronix, Beaverton, OR, USA) connected to an Apple computer.

The receptive fields of skin afferent nerves was searched with a small concentric electrically stimulating electrode. Once the electrical receptive field of a single nerve fiber was obtained and the conduction velocity was calculated, the field was probed for mechanical sensitivity using a punctuate mechanical stimulus (von Frey hair). Then the chemical sensitivity was determined. All chemicals were diluted in Krebs solution and applied via intra-arterial (i.a.) infusion into subscapular artery at a rate of 50 μl/s in a total volume of 200 μl. For every nerve studied, the vehicle was applied to ensure there was no artefactual response due to any change in mechanical force resulting from the injection. Antagonists were superfused over the tissue for 30 min and were delivered to the receptive field intra-arterially at the rate 50μl/min. Merely superfusing the Na_v1 blocking drugs (at the concentration used in this study) did not block AP conduction to the DRG, likely due to the barrier provided by the skin, and the perineural sheath protecting the axons. Therefore the small amount of drug that left the skin tissue into the superfusing solution is unlikely to have influenced the results.

Mouse Trachea

We used the isolated mouse trachea to determine the selectivity and the potency of PF05089771 on $Na_v1.7$ dependent nerve evoked cholinergic contractions (Kocmalova et al., 2017). The methods used were exactly as we previously described (Weigand et al., 2009). The neuronal responses in this isolated mouse tissue preparation are inhibited only when both $Na_v1.7$ and $Na_v1.1$ (and maybe 1.3) are blocked. In 7 experiments PF05089771 (studied in the presence of ICA121431 to block $Na_v1.1$ and 1.3) antagonized the $Na_v1.7$ responses in the isolated tracheal tissue with about the same potency as we found for compound 13 (IC_{50} of ~ 300 nM), and a maximal (>90% block) at 10 μ M. At 10 μ M neither PF05089771 alone, compound 13, nor A803467 had any effect on the neuronally evoked cholinergic contractions.

Drugs and chemicals

If not stated otherwise all drugs were purchased from Sigma-Aldrich. Chloroquine, histamine, α,β -methylene ATP, 5-HT, BAM8-22 (GenScript, Piscataway, NJ), tetrodotoxin (Alamone Laboratories Jerusalem, Israel) were dissolved in distilled water. Capsaicin and indomethacin were dissolved in ethanol. ICA121431, PF05089771 and A803467 (all Tocris Minneapolis, MN) and compound 13 (first described in WO2012004706, Almirall Laboratories, Barcelona, Spain) were dissolved in DMSO. Tetodotoxin and indomethacin were prepared as a 1mM and 30mM stock solutions, respectively; all other compounds were prepared as 10 mM stock solutions prior to being diluted in Krebs solution to their final concentrations on the day of use: 5-HT (10 μ M), A803467 (30 μ M), capsaicin (1 μ M), compound 13 (3 μ M), chloroquine (100 μ M), histamine (100 μ M), ICA121431 (10 μ M), indomethacin (3 μ M), PF05089771 (3 μ M), TTX (1 μ M), α,β -meATP (10 μ M).

Experimental Design and Statistical Analysis

The data are presented as the means \pm SEM. Response of fibers to mechanical stimulus was quantified as peak frequency - the largest number of action potentials in any 1s bin using the software TheNerveOfIt (PHOCIS, Baltimore, MD, USA). One-way ANOVA followed by Tukey's correction was used to compare quantified properties of fibers in a non-paired fashion using GraphPad Prism 7. P-value < 0.05 was considered significant.

RESULTS

Chemical and mechanical responsiveness of C-fibers in the skin

We focused this study on afferent nerve fibers that terminate in the dorsal skin and conducted action potentials at < 1 m/s, i.e. C-fibers. We studied 158 C-fibers, generally one fiber per mouse. All C-fibers found with our electrical search protocol could be activated with von Frey application to the receptive field in the skin. There is an impressive diffusion barrier to application of chemicals delivered via tissue superfusion to the receptive fields of C-fibers within the isolated dorsal skin of the mouse. We previously noted how this barrier can be circumvented by intra-arterial injection of chemicals, subsequent to cannulating the major vascular supply to the studied region of the isolated skin (Ru et al., 2017). This *ex vivo* approach offers an advantage of evaluating the activity of direct acting chemicals, but will likely underestimate the effects of those stimuli that act indirectly, e.g. via inflammatory responses, vasodilation, plasma extravasation etc.

Based on the mechanical sensitivities there were two clear C-fiber subsets. One subset was exquisitely sensitive to mechanical stimulation; the force to cause 50% maximal AP discharge (EF_{50}) averaged 3.8 ± 0.7 mN (Figure 2A). These low threshold mechanically sensitive C-fibers (C-LTMs) did not respond to any chemical stimulant that we assessed (capsaicin, CQ, 5-HT, histamine, α, β -meATP or BAM8-22). The C-LTMs comprised 20% of the total C-fiber population (Figure 2B). The rest of the C-fibers responded to von Frey stimulation with a much (~5-times) higher threshold (C-HTMs) than C-LTMs (Figure 2A). Each of the C-HTMs responded to at least one chemical stimulant assessed in this study.

We divided the C-HTMs into chloroquine-sensitive (CQ^+) and chloroquine-insensitive (CQ^-) subsets. We have previously reported that CQ activation of C-fiber in the skin, and CQ-induced scratching, depends on MRGPRA3 (Liu et al., 2009; Ru et al., 2017). In agreement with our previous data (Ru et al., 2017), we found that 24% of the C-fibers were CQ-sensitive (Figure 2B). Also in agreement with previous studies (Ru et al., 2017), nearly all (96%) of CQ^+ fibers responded with AP discharge to BAM8-22 ($n=27$) and 81% responded to histamine ($n=16$) (Figure 3). These fibers rarely responded to 5-HT (only 4 out of 29 fibers responded) or α, β -meATP (3 out of 24 responded) (Figure 3). In contrast, the vast majority of CQ^- C-fibers responded to 5-HT (76%, $n=99$) and α, β -meATP (85%,

n=45), but these nerves were only rarely activated by BAM8-22 (2 out of 53 responded) or histamine (3 out of 25 responded) (Figure 3).

The relative proportion of the 3 non-overlapping phenotypes of C-fiber: CQ⁺, CQ⁻ and C-LTMs is illustrated in Figure 2B. We did not routinely investigate capsaicin in this study, as this compound often leads to profound desensitization of the nerve, but in our previous study we found that the majority of C-fibers respond with action potential discharge to 1 μ M capsaicin (Ru et al., 2017). This is in agreement with the percentage of neurons expressing TRPV1 in the single-neuron RT-PCR data discussed below where ~70% of all neurons labeled from dorsal skin expressed TRPV1.

Interestingly, the C-LTMs did not respond to capsaicin (n=4 of 4) indicating that some of the TRPV1 negative neurons comprise C-LTMs. We infer from the stimulation profile and current knowledge (Han et al., 2013; Liu et al., 2009; Ru et al., 2017), that CQ⁺ C-fibers in the skin represent itch (scratch-evoking) C-fibers, whereas cutaneous capsaicin-sensitive CQ⁻ C-fibers comprise pain-evoking nociceptors, and C-LTMs transduce non-painful tactile signals (Olausson et al., 2002; Vallbo et al., 1999). C-LTMs may also contribute to pain in pathological states (Seal et al., 2009).

Conduction velocity and peak frequency

We observed similar average conduction velocities for all three categories of skin C-fibers; itch fibers averaged 0.55 ± 0.03 m.s⁻¹ (n=24), nociceptive fibers averaged 0.58 ± 0.01 m.s⁻¹ (n=58), and C-LTMs averaged 0.64 ± 0.04 m.s⁻¹ (n=11) (Figure 2C). In terms of peak frequency induced by mechanical probing of the skin, itch C-fibers fired with the peak frequency of 12.8 ± 0.6 Hz (n=24) which was modestly, but significantly less than nociceptive C-fibers (15.7 ± 0.6 Hz, n=58) or C-LTMs (20.9 ± 1.2 Hz, n=19) (Figure 2D).

Expression of voltage-gated sodium channels

Using retrograde labeling and single cell RT-PCR we evaluated the expression of a subunits of neuronal Na_v1 channels in 74 skin-specific dorsal root ganglia neurons. In order to discriminate between CQ⁺ itch C-fiber neurons and nociceptive neurons, we considered the expression of MRGPRA3 mRNA as a marker of itch fiber neurons and the expression of TRPV1 *but not* MRGPRA3 mRNA as a marker of nociceptors (Liu et al., 2009). C-LTMs were found to be capsaicin-negative so

we also included in Figure 4 data from non-TRPV1 expressing neurons. Unfortunately, we did not find a reliable marker for C-LTMs, so the TRPV1-negative neurons likely comprise C-LTM neurons as well as other TRPV1-negative neurons including non-nociceptive A-fiber neurons. Of 74 evaluated neurons 24% were MRGPRA3-positive; this corresponds quantitatively with the CQ-sensitive population of fibers discussed above. As expected, the percentage of MRGPRA3 expressing neurons that innervate the skin was much greater than previously reported ~5% of general DRG neuronal population (Liu et al., 2009). The vast majority of the itch and nociceptive neurons expressed Na_v1.7, 1.8 and 1.9. In addition, about 30% of the nociceptive neurons expressed Na_v1.6 and a smaller subpopulation of neurons expressed Na_v1.1, 1.2, and 1.3. About 20% of the MRGPRA3 itch neurons expressed Na_v1.6, with most of the other Na_v1s rarely expressed. The TRPV1-negative neurons were, as might be expected, more heterogeneous with the major distinction from the MRGPRA3 and TRPV1-positive populations being that a smaller percentage expressed Na_v1.8 or Na_v1.9, and a larger percentage expressing Na_v1.1 (Figure 4).

Pharmacological blocking of voltage-gated sodium channels in the skin

We evaluated the effect of Na_v1 blocking drugs added intra-arterially to the receptive field of cutaneous primary afferent nerve fibers on the action potential discharge in response to mechanical stimulation. We used concentrations of inhibitors expected to cause near complete blockade of the respective channels, based on our previous study with mouse isolated airway tissue (Kocmalova et al., 2017).

Tetrodotoxin-sensitivity

TTX (1 μM) abolished action potential discharge in all C-LTMs (n=8) and all nociceptors (n=65). In contrast 4 of 19 of itch C-fibers responded normally when TTX-sensitive channels were blocked (n=19) (Figure 5).

TTX-sensitive channel subtypes involved in action potential discharge

We used 2 selective Na_v1.7 blockers PF05089771 (3 μM, n=36) and Compound 13 (3 μM, n =40), the results were similar for both of them so we pooled the data. The selectivity of Compound 13 is reported in Kocmalova et al. (2017) and the selectivity of PF05089771 is reported in Alexandrou et.al

(2016). We also evaluated PF05089771 in our previously described $\text{Na}_V1.7$ assay using neuronally evoked cholinergic contractions of mouse trachea and found that, like Compound 13, the IC_{50} of this state-dependent inhibitor was ~ 300 nM (about 10-fold less potent than TTX) with maximal block occurring at 3-10 μM . It was recently reported that PF05089771 can inhibit the TTX-resistant $\text{Na}_V1.8$ current in human isolated DRG neurons (Zhang et al., 2017), so we have examined the effects of PF05089771 on TTX-sensitive and TTX-resistant sodium current (I_{Na}) in voltage-clamped isolated mouse DRG neurons. In 3 experiments, bath perfusion of PF05089771 (3 μM) for 5 mins blocked the TTX-sensitive I_{Na} by 54, 85 and 92%. In two of the three neurons where there was a notable TTX-resistant $\text{Na}_V1.8$ -like I_{Na} , PF05089771 had essentially no inhibitory effect; at -20 mV there was 655 pA and 350 pA in the absence of drug and 631 pA and 351 pA in the presence of drug, respectively.

The $\text{Na}_V1.7$ blockers abolished the responses of 64% of the nociceptive C-fibers (n=42), 42% of itch C-fibers (n=19), but only 18% of C-LTMs (n=11) (Figure 6).

The $\text{Na}_V1.1/1.2/1.3$ blocker ICA121431 (10 μM) alone had no effect on any C-fiber studied (n=13). In 4 experiments where a C-LTM was not blocked by $\text{Na}_V1.7$ blockers alone, they were each silenced by the further addition of ICA121431. Among the 8 nociceptive C-fibers that were not abolished by $\text{Na}_V1.7$ blockers, adding ICA121431 abolished the response in 4 of the fibers. In contrast, further addition of ICA12143 had no effect on $\text{Na}_V1.7$ blocker resistant itch C-fibers (n=4). These data are tabulated in Table 1.

TTX-insensitive channel ($\text{Na}_V1.8$) involved in action potential discharge

The $\text{Na}_V1.8$ blocker A803467 (30 μM) alone had no effect on the activity of any C-fiber studied (n=15). However, both itch and nociceptive C-fibers not silenced by $\text{Na}_V1.7$ blockade, were silenced by the further addition of A803467 (4/4 itch fibers, 4/4 nociceptive fibers) (Table 1).

DISCUSSION

The results indicate that within the cutaneous compartment of the C57BL/6J mouse dorsal thorax, selectively blocking Na_v1.7 will silence AP discharge in about 40-60% of itch C-fibers and nociceptive C-fibers, but only rarely will it silence C-LTMs. A combination of a Na_v1.7 and a 1.8 blocker would be predicted to block virtually all itch and nociceptive C-fibers and therefore eliminate pruritogen or algogenic evoked C-fiber activation in this region of the skin. These therapeutic conclusions need to be tempered by the fact that the data was obtained from healthy skin and the activity and profile of Na_v channels may change in disease (Dib-Hajj et al., 2010).

Using an *ex-vivo* dorsal skin-nerve preparation we were able to characterize three non-overlapping subsets of C-fibers in the skin of the dorsal thorax. All C-fibers found by using a search paradigm where a small concentric electrode was used to probe the skin, were mechanically sensitive to punctate stimulation with von Frey fibers. Based on the mechanical sensitivity, the anticipated two subpopulations of cutaneous C-fibers emerged; namely C-LTMs and C-HTMs with the later far outnumbering the former. The C-LTMs were unresponsive to all the chemical stimuli that we studied. Based on their chemical activation, we were able to distinguish between two subsets of C-HTM fibers. One subset was strongly activated by CQ (24.2%) versus the larger subset that did not respond to CQ. We previously noted that the majority of both of these subsets will respond to capsaicin, but the CQ-sensitive fibers selectively responded to three additional pruritic stimuli, namely cutaneous allergen challenge, histamine, and the MrgprC11 agonist BAM8-22 (Ru et al., 2017). Considering these data, along with the observation that selective deletion of CQ-sensitive neurons in the mouse DRG strongly reduced scratching to a variety of stimuli (Han et al., 2013), we *ostensibly* termed the CQ-sensitive nerves in the skin “itch C-fibers”. That the pruritogen (CQ, histamine, allergen, BAM8-22) *insensitive* C-fibers in contrast, responded strongly to algogenic chemicals (5-HT, α , β -meATP, capsaicin), is the basis for referring to them as cutaneous nociceptive (likely pain evoking) C-fibers. The physiological function of the C-LTMs in the dorsal skin remain ambiguous (Loken et al., 2009; Olausson et al., 2002; Seal et al., 2009; Vallbo et al., 1999). These three subsets of cutaneous C-fibers are likely a gross oversimplification, as it is reasonable to assume the two broad categories of C-HTMs comprise phenotypical subsets if other stimuli were evaluated, see Dubin and Patapoutian (2010).

Several previous studies in both laboratory animals and humans have observed mechanically silent C-fibers in the skin (Kress et al., 1992; Lawson et al., 2008; Weidner et al., 1999). In an *ex vivo* adult mouse skin-nerve preparations akin to what was used here, Lawson et al. noted that about 10% of the cutaneous C-fibers were mechanically insensitive (Lawson et al., 2008). This study, however, focused mainly on the skin of the hind paw. The search paradigm was different between the two studies as well. In the present study, we only evaluated C-fibers in which the receptive field in the skin was first identified with a small concentric stimulating electrode applied locally to the skin. In any event, it can be concluded that the vast majority of cutaneous C-fibers in mouse skin are mechanically sensitive.

The single cell RT-PCR analysis revealed that neurons with a presumed nociceptive phenotype (expressing TRPV1 but not MrgprA3) as well as those with a presumed itch phenotype (MrgprA3 expressing) express a similar profile of Na_v1 α subunits genes with NaV 1.7, 1.8 and 1.9 expressed the most frequently. These data are in keeping with RNAseq analysis of MrgprA3 expressing DRG neurons where Na_v 1.7, 1.8 and 1.9 were by far the dominant Na_v subunits expressed (Usoskin et al., 2015). Our analysis indicated that about 60-70% of all neurons labeled from the dorsal region of mouse skin expressed TRPV1. This is a much larger percentage than observed in studies using immuno-histochemistry to evaluate TRPV1 expression in mouse and rat cutaneous neurons (Lawson et al., 2008; Tsukagoshi et al., 2006). It is possible that the mRNA is not translated in all neurons, however the RT-PCR data are in keeping with our previous observation that the majority of C-fibers terminating in this region of the skin respond strongly with action potential discharge when capsaicin is applied to the cutaneous receptive field (Ru et al., 2017).

It has previously been noted that the Na_v1 subtypes supporting AP discharge may be different between the terminal region of the nerve within a tissue versus the conducting region of the axons in the extrinsic nerves (Brock et al., 1998; Kollarik et al., 2018). Therefore, by focusing on the effect of selective Na_v1 blockers delivered intra-arterially to the receptive field in the isolated skin we were able to, for the first time, characterize the Na_v1 subtypes supporting AP generation within the cutaneous tissue compartment. Although other studies indicate that TTX-resistant channels may be more

dominant near and within the peripheral tissues than along the axons within the extrinsic nerves (Klein et al., 2017), it was notable that TTX selectively applied to the skin compartment was effective in silencing all C-LTMs as well as the vast majority of C-HTMs.

Selective Na_v1.7 antagonism alone blocked the APs in only a minority (~40%) of skin itch C-fibers. Although the Na_v1.8 blocker alone had no effect on itch C-fibers, in itch C-fibers that were not blocked by a Na_v1.7 blocker adding the Na_v1.8 blocker abolished the response. These data support the hypothesis that when drugs are limited to the cutaneous compartment, the combination of a Na_v1.7 and Na_v1.8 blockade will be more effective in inhibiting itch than blocking either channel alone.

A major role for Na_v1.7 in itch has previously been inferred from *in vivo* studies where genetically deleting Na_v1.7 virtually abolished scratching to histamine (Gingras et al., 2014). This was a greater inhibitory effect that would be predicted from the present study. This raises four possible explanations; first, the drugs did not completely block Na_v1.7 channels; second, that blocking some 40% of itch C-fibers is sufficient to inhibit all evoked scratching in the mouse; third, deleting Na_v1.7 led to the modulation of other relevant genes, e.g. see (Minett et al., 2015); and fourth, blocking Na_v1.7 in extra-cutaneous aspects of the nerve is more effective in inhibiting AP conduction in itch C-fibers than what is observed within the skin. Sulfonamide based Na_v1.7 blockers (a class of Na_v1.7 antagonists used also in our study) administered *systemically* prior to histamine intradermal injection reduced scratching by up to 85% (Graceffa et al., 2017; Kornecook et al., 2017; La et al., 2017).

A similar case can be made for cutaneous pain. The majority (65%) of nociceptive C-fibers were silenced by the Na_v1.7 blockers. In the remaining fibers blocking either Na_v1.8 or other TTX-sensitive Na_v1s in addition to Na_v1.7 silenced the nerves (none responded in presence of TTX). This was likely due to the presence of Na_v1.1 and/or 1.6 in a subpopulation of these nerves. This observation is in general agreement with the findings of Kornecook et al. (2017) who noted that ~50% of the TTX-sensitive AP firing in the of tibial/saphenous nerves evoked by focal heat stimulation of hind paw was blocked by an Na_v1.7 blocker. Likewise, intraplantar injection of capsaicin evoked licking behavior is inhibited by about 50- 75% with Na_v1.7 blocking drugs (Graceffa et al., 2017; Kornecook et al., 2017).

The firmness of our conclusions depends on the selectivity of the Na_v1 blockers studied. The selectivity can be challenged by the fact that large concentration of Na_v1 blockers are required to abolish neural activation in isolated tissues relative to their potencies at inhibiting sodium currents under idealized patch clamp conditions. Data we obtained previously (and in the present study) with the mouse isolated trachea provides some insight about drug selectivity that is relevant to the present study (Kocmalova et al., 2017). The neuronally-evoked cholinergic contraction of the mouse trachea is dependent on a redundant role of Na_v1.7, Na_v1.1 and Na_v1.3 (Kocmalova et al., 2017). Accordingly, TTX abolishes the responses as does the combination of a Na_v1.7 blocker and ICA12143 (to block Na_v1.1 and 1.3). Alone, the Na_v1.7 blockers used in the present study have no effect up to 10 μM on the neuronal responses in the trachea, indicating their lack of effect on Na_v1.1 and 1.3. Likewise, the Na_v1.1/1.2/1.3 blocker ICA12143 has no effect on neuronal tracheal contractions up to 10 μM, revealing its lack of effect of ICA12143 on Na_v1.7. When Na_v1.1 and 1.3 were blocked with ICA12143, then Compound 13 or PF05089771 blocked the remaining Na_v1.7 response with an IC₅₀ of ~ 300 nM and complete blockade at 1-10 μM. It must be kept in mind however that PF089771 will likely inhibit Na_v1.6 in our tissue, and this channel was expressed in a small subset of pain and itch neurons. With these caveats in mind, our data support the conclusion that combination of topically applied Na_v1.7 and Na_v1.8 blocker would almost certainly reduced acute pain and itch emanating from the skin of the mouse.

ACKNOWLEDGMENTS

We acknowledge the excellent technical assistance of Ms Sonya Meeker.

AUTHORSHIP CONTRIBUTIONS

Participated in research design: Jurcakova, Ru, Kollarik, Sun, Krajewski and Udem

Conducted experiments: Jurcakova, Ru and Sun

Performed data analysis: Jurcakova, Ru, Sun and Udem

Wrote or contributed to the writing of the manuscript: Jurcakova, Kollarik and Udem

REFERENCES

- Alexandrou AJ, Brown AR, Chapman ML, Estacion M, Turner J, Mis MA, Wilbrey A, Payne EC, Gutteridge A, Cox PJ, Doyle R, Printzenhoff D, Lin Z, Marron BE, West C, Swain NA, Storer RI, Stupple PA, Castle NA, Hounshell JA, Rivara M, Randall A, Dib-Hajj SD, Krafte D, Waxman SG, Patel MK, Butt RP and Stevens EB (2016) Subtype-Selective Small Molecule Inhibitors Reveal a Fundamental Role for Nav1.7 in Nociceptor Electrogenesis, Axonal Conduction and Presynaptic Release. *PLoS One* **11**(4): e0152405.
- Brock JA, McLachlan EM and Belmonte C (1998) Tetrodotoxin-resistant impulses in single nociceptor nerve terminals in guinea-pig cornea. *J Physiol* **512** (Pt 1): 211-217.
- Brozmanova M, Mazurova L, Ru F, Tatar M, Hu Y, Yu S and Kollarik M (2016) Mechanisms of the adenosine A2A receptor-induced sensitization of esophageal C fibers. *Am J Physiol Gastrointest Liver Physiol* **310**(3): G215-223.
- Dib-Hajj SD, Cummins TR, Black JA and Waxman SG (2010) Sodium channels in normal and pathological pain. *Annu Rev Neurosci* **33**: 325-347.
- Dubin AE and Patapoutian A (2010) Nociceptors: the sensors of the pain pathway. *J Clin Invest* **120**(11): 3760-3772.
- Emery EC, Luiz AP, Sikandar S, Magnusdottir R, Dong X and Wood JN (2016) In vivo characterization of distinct modality-specific subsets of somatosensory neurons using GCaMP. *Sci Adv* **2**(11): e1600990.
- Gingras J, Smith S, Matson DJ, Johnson D, Nye K, Couture L, Feric E, Yin R, Moyer BD, Peterson ML, Rottman JB, Beiler RJ, Malmberg AB and McDonough SI (2014) Global Nav1.7 knockout mice recapitulate the phenotype of human congenital indifference to pain. *PLoS One* **9**(9): e105895.
- Graceffa RF, Boezio AA, Able J, Altmann S, Berry LM, Boezio C, Butler JR, Chu-Moyer M, Cooke M, DiMauro EF, Dineen TA, Feric Bojic E, Foti RS, Fremeau RT, Jr., Guzman-Perez A, Gao H, Gunaydin H, Huang H, Huang L, Ilch C, Jarosh M, Kornecook T, Kreiman CR, La DS, Ligutti J, Milgram BC, Lin MJ, Marx IE, Nguyen HN, Peterson EA, Rescourio G, Roberts J, Schenkel L, Shimanovich R, Sparling BA, Stellwagen J, Taborn K, Vaida KR, Wang J, Yeoman J, Yu V, Zhu D, Moyer BD and Weiss MM (2017) Sulfonamides as Selective NaV1.7 Inhibitors:

- Optimizing Potency, Pharmacokinetics, and Metabolic Properties to Obtain Atropisomeric Quinolinone (AM-0466) that Affords Robust in Vivo Activity. *J Med Chem* **60**(14): 5990-6017.
- Han L, Ma C, Liu Q, Weng HJ, Cui Y, Tang Z, Kim Y, Nie H, Qu L, Patel KN, Li Z, McNeil B, He S, Guan Y, Xiao B, Lamotte RH and Dong X (2013) A subpopulation of nociceptors specifically linked to itch. *Nat Neurosci* **16**(2): 174-182.
- Klein AH, Vyshnevskaya A, Hartke TV, De Col R, Mankowski JL, Turnquist B, Bosmans F, Reeh PW, Schmelz M, Carr RW and Ringkamp M (2017) Sodium Channel Nav1.8 Underlies TTX-Resistant Axonal Action Potential Conduction in Somatosensory C-Fibers of Distal Cutaneous Nerves. *J Neurosci* **37**(20): 5204-5214.
- Kocmalova M, Kollarik M, Canning BJ, Ru F, Adam Herbstsomer R, Meeker S, Fonquerna S, Aparici M, Miralpeix M, Chi XX, Li B, Wilenkin B, McDermott J, Nisenbaum E, Krajewski JL and Udem BJ (2017) Control of Neurotransmission by Nav1.7 in Human, Guinea Pig, and Mouse Airway Parasympathetic Nerves. *J Pharmacol Exp Ther* **361**(1): 172-180.
- Kollarik M, Sun H, Herbstsomer RA, Ru F, Kocmalova M, Meeker SN and Udem BJ (2018) Different role of tetrodotoxin-sensitive voltage-gated sodium channel (Nav1) subtypes in action potential initiation and conduction in vagal airway nociceptors. *J Physiol*.
- Kornecook TJ, Yin R, Altmann S, Be X, Berry V, Ilch CP, Jarosh M, Johnson D, Lee JH, Lehto SG, Ligutti J, Liu D, Luther J, Matson D, Ortuno D, Roberts J, Taborn K, Wang J, Weiss MM, Yu V, Zhu DXD, Fremeau RT, Jr. and Moyer BD (2017) Pharmacologic Characterization of AMG8379, a Potent and Selective Small Molecule Sulfonamide Antagonist of the Voltage-Gated Sodium Channel Nav1.7. *J Pharmacol Exp Ther* **362**(1): 146-160.
- Kress M, Koltzenburg M, Reeh PW and Handwerker HO (1992) Responsiveness and functional attributes of electrically localized terminals of cutaneous C-fibers in vivo and in vitro. *J Neurophysiol* **68**(2): 581-595.
- Kwong K, Carr MJ, Gibbard A, Savage TJ, Singh K, Jing J, Meeker S and Udem BJ (2008) Voltage-gated sodium channels in nociceptive versus non-nociceptive nodose vagal sensory neurons innervating guinea pig lungs. *J Physiol* **586**(5): 1321-1336.
- La DS, Peterson EA, Bode C, Boezio AA, Bregman H, Chu-Moyer MY, Coats J, DiMauro EF, Dineen TA, Du B, Gao H, Graceffa R, Gunaydin H, Guzman-Perez A, Fremeau R, Jr., Huang X, Ilch C, Kornecook TJ, Kreiman C, Ligutti J, Jasmine Lin MH, McDermott JS, Marx I, Matson DJ,

- McDonough SI, Moyer BD, Nho Nguyen H, Taborn K, Yu V and Weiss MM (2017) The discovery of benzoxazine sulfonamide inhibitors of Nav1.7: Tools that bridge efficacy and target engagement. *Bioorg Med Chem Lett* **27**(15): 3477-3485.
- Lai J, Porreca F, Hunter JC and Gold MS (2004) Voltage-gated sodium channels and hyperalgesia. *Annu Rev Pharmacol Toxicol* **44**: 371-397.
- Lawson JJ, McIlwrath SL, Woodbury CJ, Davis BM and Koerber HR (2008) TRPV1 unlike TRPV2 is restricted to a subset of mechanically insensitive cutaneous nociceptors responding to heat. *J Pain* **9**(4): 298-308.
- Liu Q, Tang Z, Surdenikova L, Kim S, Patel KN, Kim A, Ru F, Guan Y, Weng HJ, Geng Y, Udem BJ, Kollarik M, Chen ZF, Anderson DJ and Dong X (2009) Sensory neuron-specific GPCR Mrgprs are itch receptors mediating chloroquine-induced pruritus. *Cell* **139**(7): 1353-1365.
- Loken LS, Wessberg J, Morrison I, McGlone F and Olausson H (2009) Coding of pleasant touch by unmyelinated afferents in humans. *Nat Neurosci* **12**(5): 547-548.
- Minett MS, Pereira V, Sikandar S, Matsuyama A, Lalignier S, Kanellopoulos AH, Mancini F, Iannetti GD, Bogdanov YD, Santana-Varela S, Millet Q, Baskozos G, MacAllister R, Cox JJ, Zhao J and Wood JN (2015) Endogenous opioids contribute to insensitivity to pain in humans and mice lacking sodium channel Nav1.7. *Nat Commun* **6**: 8967.
- Muroi Y, Ru F, Kollarik M, Canning BJ, Hughes SA, Walsh S, Sigg M, Carr MJ and Udem BJ (2011) Selective silencing of Na(V)1.7 decreases excitability and conduction in vagal sensory neurons. *J Physiol* **589**(Pt 23): 5663-5676.
- Olausson H, Lamarre Y, Backlund H, Morin C, Wallin BG, Starck G, Ekholm S, Strigo I, Worsley K, Vallbo AB and Bushnell MC (2002) Unmyelinated tactile afferents signal touch and project to insular cortex. *Nat Neurosci* **5**(9): 900-904.
- Rozen S and Skaletsky H (2000) Primer3 on the WWW for general users and for biologist programmers. *Methods Mol Biol* **132**: 365-386.
- Ru F, Sun H, Jurcakova D, Herbstsomer RA, Meixong J, Dong X and Udem BJ (2017) Mechanisms of pruritogen-induced activation of itch nerves in isolated mouse skin. *J Physiol* **595**(11): 3651-3666.
- Ru F, Surdenikova L, Brozmanova M and Kollarik M (2011) Adenosine-induced activation of esophageal nociceptors. *Am J Physiol Gastrointest Liver Physiol* **300**(3): G485-493.

- Seal RP, Wang X, Guan Y, Raja SN, Woodbury CJ, Basbaum AI and Edwards RH (2009) Injury-induced mechanical hypersensitivity requires C-low threshold mechanoreceptors. *Nature* **462**(7273): 651-655.
- Surdenikova L, Ru F, Nassenstein C, Tatar M and Kollarik M (2012) The neural crest- and placodes-derived afferent innervation of the mouse esophagus. *Neurogastroenterol Motil* **24**(10): e517-525.
- Tsukagoshi M, Goris RC and Funakoshi K (2006) Differential distribution of vanilloid receptors in the primary sensory neurons projecting to the dorsal skin and muscles. *Histochem Cell Biol* **126**(3): 343-352.
- Usoskin D, Furlan A, Islam S, Abdo H, Lonnerberg P, Lou D, Hjerling-Leffler J, Haeggstrom J, Kharchenko O, Kharchenko PV, Linnarsson S and Ernfors P (2015) Unbiased classification of sensory neuron types by large-scale single-cell RNA sequencing. *Nat Neurosci* **18**(1): 145-153.
- Vallbo AB, Olausson H and Wessberg J (1999) Unmyelinated afferents constitute a second system coding tactile stimuli of the human hairy skin. *J Neurophysiol* **81**(6): 2753-2763.
- Weidner C, Schmelz M, Schmidt R, Hansson B, Handwerker HO and Torebjork HE (1999) Functional attributes discriminating mechano-insensitive and mechano-responsive C nociceptors in human skin. *J Neurosci* **19**(22): 10184-10190.
- Weigand LA, Myers AC, Meeker S and Udem BJ (2009) Mast cell-cholinergic nerve interaction in mouse airways. *J Physiol* **587**(Pt 13): 3355-3362.
- Zhang X, Priest BT, Belfer I and Gold MS (2017) Voltage-gated Na(+) currents in human dorsal root ganglion neurons. *Elife* **6**.

FOOTNOTES

Danica Jurcakova was partially supported by APVV-15-0163 and VEGA 1/0306/18 (Department of Education, Slovakia).

LEGENDS FOR FIGURES

Figure 1

Mouse skin-nerve *ex vivo* preparation. A. Location of skin used for retrograde labeling and electrophysiological recordings. B. The dorsal root ganglia (DRG) - spinal nerve–skin preparation. The skin (1) is pinned dermis side up in the tissue chamber, the T9 thoracic nerve (2) passes through a hole sealed with Vaseline into the recording chamber where the T9 DRG (3) is positioned and pinned at the distal end. An extracellular recording electrode (4) has the tip positioned in the dorsal root ganglia. The tissue and the recording chamber are separately superfused with warm Krebs solution. Mechanical stimuli (von Frey hairs) are applied to the dermis (corium) side of the skin. Chemicals are delivered via cannulated right subscapular artery (5) connected to PE tubing (edited from Ru et al., 2017).

Figure 2

Properties of chloroquine-sensitive C-HTMs (CQ+, itch fibers), CQ-insensitive C-HTM fibers (CQ-; nociceptors) and low-threshold mechanosensitive C-fibers (C-LTMs). A. Mechanical sensitivity determined as peak frequency obtained by punctual mechanical stimulation with von Frey hair in mN. The force required to evoke a 50% response was about 10-fold less for C-LTMs than C-HTMs ($p < 0.001$). B. Proportion of CQ+, CQ- and C-LTMs fibers in the dorsal mouse skin ($n=66$). C. Conduction velocity in m/s. D. Peak frequency in Hz (CQ+ vs CQ-: $p=0.024$, CQ+ vs C-LTMs: $p < 0.001$; CQ- vs C-LTMs: $p < 0.001$). One-way ANOVA followed by Tukey's test was used to determine p-values. In A, C and D, data are presented as means \pm SEM of individual fibers studied.

Figure 3

Chemical responsiveness of C-fibers innervating the mouse skin.

A. Representative traces showing the action potential discharge evoked in response to chemical or mechanical stimulation. **B.** The proportion of the three subtypes of C-fibers studied that respond to various chemicals. Open squares are C-HTMs that respond to CQ (itch fibers); the black squares are C-HTM fibers those that do not respond to CQ (nociceptors); and the shaded bars are C-LTMs. Among the chloroquine-sensitive (CQ+; itch) C-fibers (open bars), 26 of 27 responded to BAM8-22,

13 of 16 responded to histamine (HA), but only 4 of 29 to 5-HT and 3 of 24 to α,β -methylene ATP (α,β -meATP). On the other hand, CQ-insensitive high-mechanical threshold C-fibers (CQ-; nociceptors) (closed bars) responded likely to α,β -meATP (38 of 45 fibers tested) and 5-HT (75 of 99) and only rarely to HA (3 of 25) or BAM8-22 (2 of 53). Note: none of the low-threshold mechanosensitive C-fibers (C-LTMs) responded to any of assessed chemical stimuli (n=14). Response to chemical stimuli is denoted above the columns as number of action potentials (APs; mean \pm SEM).

Figure 4

Co-expression of sodium channels subtypes (Na_v1s) in dorsal root ganglia neurons

innervating dorsal mouse skin. Top: Gene expression wheels. Each box represents a single neuron (depicted on the right). For each neuron the expression or lack thereof of 7 Na_v s are shown by the filled in color (color-coded on right), e.g. $Na_v1.7$ expression is denoted as red in the third wheel, note that all but three nociceptors and all but three itch fibers expressed $Na_v1.7$. Neurons were divided based on the expression of nociceptor marker TRPV1 and chloroquine-receptor (MRGPRA3) into 2 subpopulations presumably representing pain- evoking nociceptors (TRPV1+ and MRGPRA3-) and itch (scratch-evoking) C-fibers (MRGPRA3+). Virtually all of these fibers express $Na_v1.9$ and $Na_v1.8$. This phenomenon was not observed in other (TRPV1- and MRGPRA3-) neurons that are included in the figure for comparison.

Bottom: Relative expression of Na_v s transcripts in 3 identified subpopulations of dorsal root ganglia neurons.

Figure 5

Effect of tetrodotoxin (TTX) on C-fibers innervating the mouse skin.

A. Percentage of chloroquine-sensitive (CQ+; itch fibers), CQ-insensitive high-mechanical threshold C-fibers (CQ-; nociceptors) and low threshold mechanosensitive C-fibers (C-LTMs) blocked by TTX (1 μ M). **B.** Representative traces of effect of TTX on CQ-sensitive (CQ+; itch fibers), CQ-insensitive high-mechanical threshold C-fibers (CQ-; nociceptors) and low threshold mechanosensitive C-fibers (C-LTMs) stimulated with von Frey hair, showing TTX-sensitive fibers and a TTX-resistant itch fiber.

For CQ-sensitive C-fibers (CQ+; itch fibers) examples of a TTX-sensitive fiber and a TTX-resistant fiber are shown.

Figure 6

Effect of Na_v1.7-subtype selective blockers on C-fibers innervating the mouse skin.

A. Percentage of chloroquine-sensitive (CQ+; itch fibers), CQ-insensitive high-mechanical threshold C-fibers (CQ-; nociceptors) and low threshold mechanosensitive C-fibers (C-LTMs) blocked by Na_v1.7 blockers (pooled data for compound 13, 3μM and PF05089771, 3μM). **B.** Representative traces of mechanical (von Frey) activation of CQ-sensitive (CQ+; itch fiber) being silenced by the Na_v1.7 blocker, and another CQ+ fiber where blocking Na_v1.7 had no effect, but adding the Na_v1.8 blocker A803467 silenced the fiber (A803467 alone does not inhibit the itch fibers); note that following treatment with PF05089771 another mechanically-sensitive fiber appeared with a smaller amplitude—this fiber was also silenced by the addition of A803467).

TABLES

Table 1

Effect of sodium channel blocking on C-fibers innervating the mouse skin

	% of C-fibers blocked ^a		
	itch fibers ^b	nociceptors ^c	C-LTMs ^d
TTX	78.9% (19) ^e	100% (65)	100% (8)
Na _v 1.7 blockers ^f	42.1% (19)	63.6% (44)	21.4% (14)
ICA121431	0% (4)	0% (5)	0% (4)
A803467	0% (4)	0% (7)	0% (4)
% of Na_v1.7 blocker - resistant fibers			
Na _v 1.7 blockers plus ICA121431	0% (4)	50% (8)	100% (4)
Na _v 1.7 blockers plus A803467	100% (4)	100% (4)	50% (4)

^a mechanical response to punctuate stimulation with von Frey hairs was evaluated before and after incubation with Na_v blockers. Fiber was considered to be blocked if it was unable to fire action potentials after applying adequate mechanical and chemical stimulus.

^b itch fibers are defined as high-mechanical threshold chloroquine-sensitive C-fibers

^c nociceptors are defined as high-mechanical threshold chloroquine-insensitive C-fibers

^d low mechanical threshold C-fibers

^e total number of experiments

^f pooled data for Na_v1.7 blockers PF05089771 (3μM) and Compound 13 (3μM)

Table 2

Primer sequences for single cell RT-PCR

gene	primer	sequence (5` to 3`)	product size
β-actin	forward	GTGGGAATGGGTCAGAAGG	302 bp
	reverse	GAGGCATACAGGGACAGCA	
MRGPRA3	forward	CGACAATGACACCCACAACAA	150 bp
	reverse	GGAAGCCAAGGAGCCAGAAC	
TRPV1	forward	GCTGCTAACGGGGACTTCTT	285 bp
	reverse	CTTCAGTGTGGGGTGGAGTT	
Na _v 1.1	forward	AGACAGCATCAGGAGGAAGG	118 bp
	reverse	GGAGAACAGGGAACCACGA	
Na _v 1.2	forward	CATTTTCGGCTCATTCTTCA	305 bp
	reverse	CATCTCTTGGCTCTGGTCGT	
Na _v 1.3	forward	AGACAGAGGGAGCACTTGGA	200 bp
	reverse	CTATTGCGTCTTGGGGAAAA	
Na _v 1.6	forward	AGGCAGCAAAGACAAACTGG	157 bp
	reverse	GCAGCACTTGAACCTCTGG	
Na _v 1.7	forward	ATGCTCTTCTTTGCGGTTTC	381 bp
	reverse	CCTGCTCTTTTCGGCTTCTT	
Na _v 1.8	forward	CAATCCGACCCTTACAACCA	147 bp
	reverse	AAAGACCCCGTCATCCAAG	
Na _v 1.9	forward	CAGCTTTGGCTGGTCTTTTC	228 bp
	reverse	TTCTCCTTGGCCTCTGTCTC	

FIGURES

Figure 1

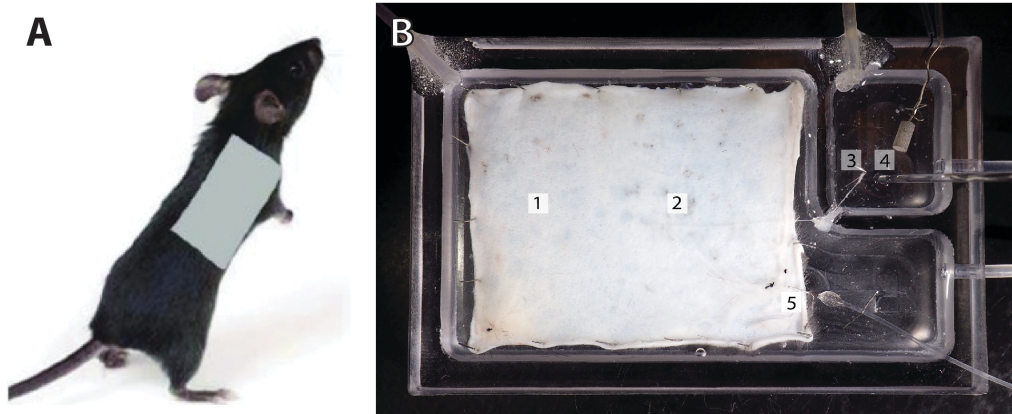


Figure 2

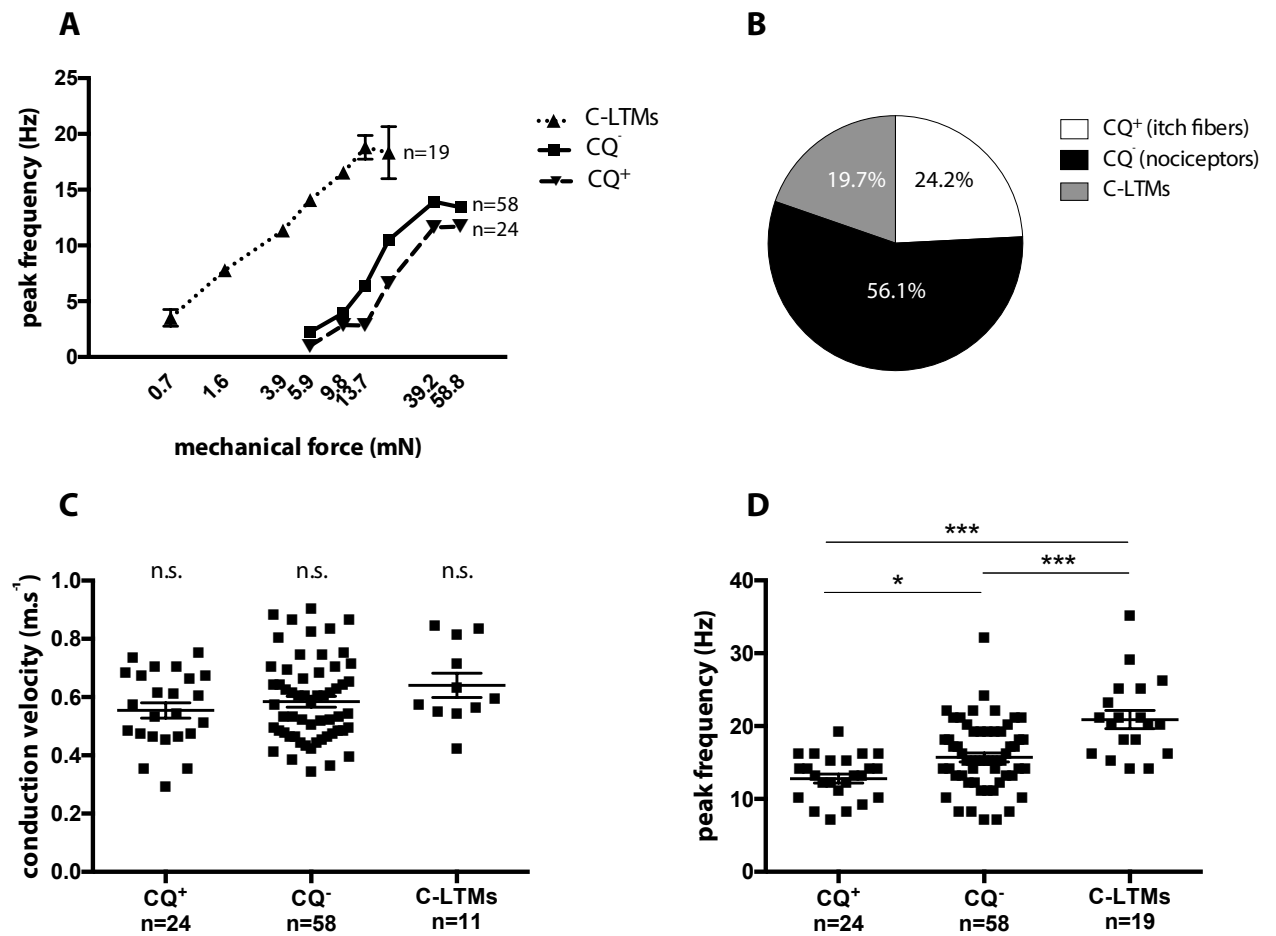


Figure 3

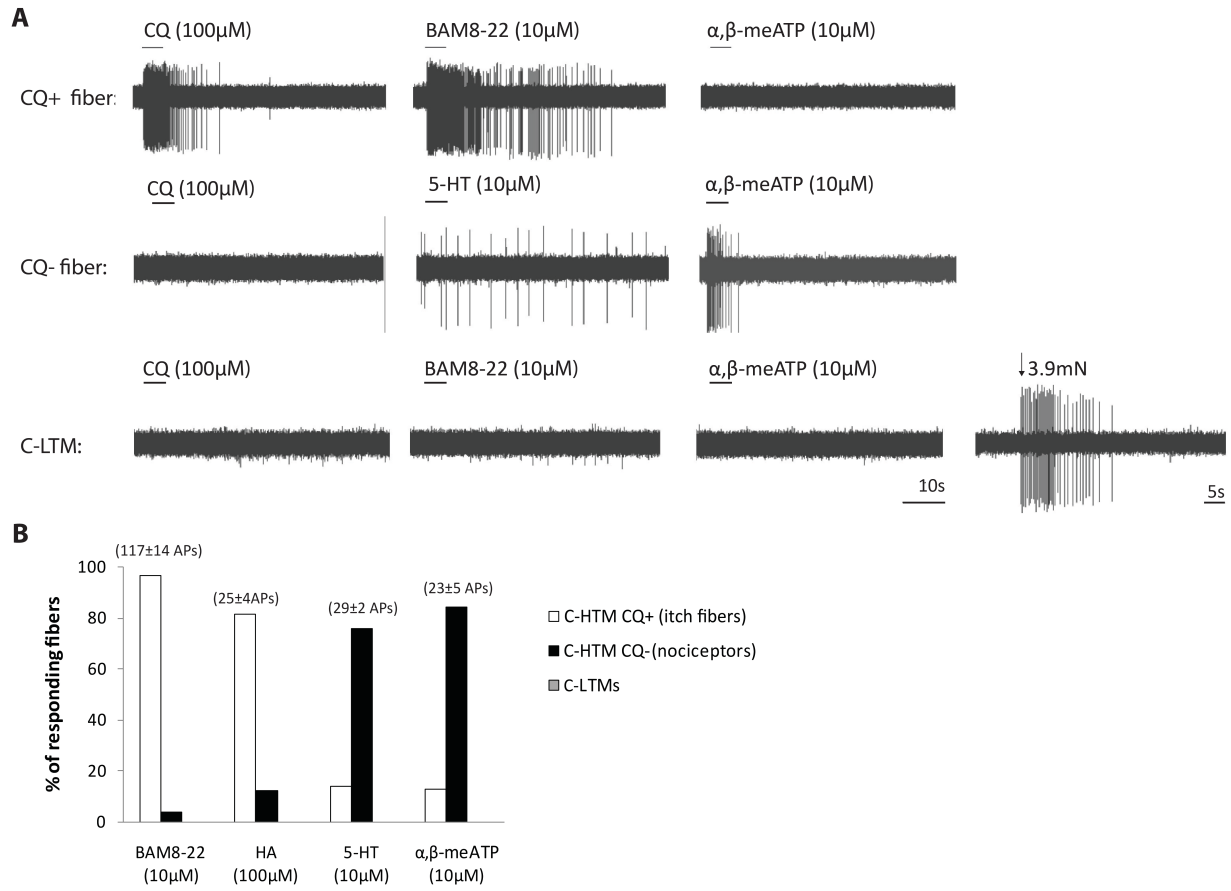


Figure 4

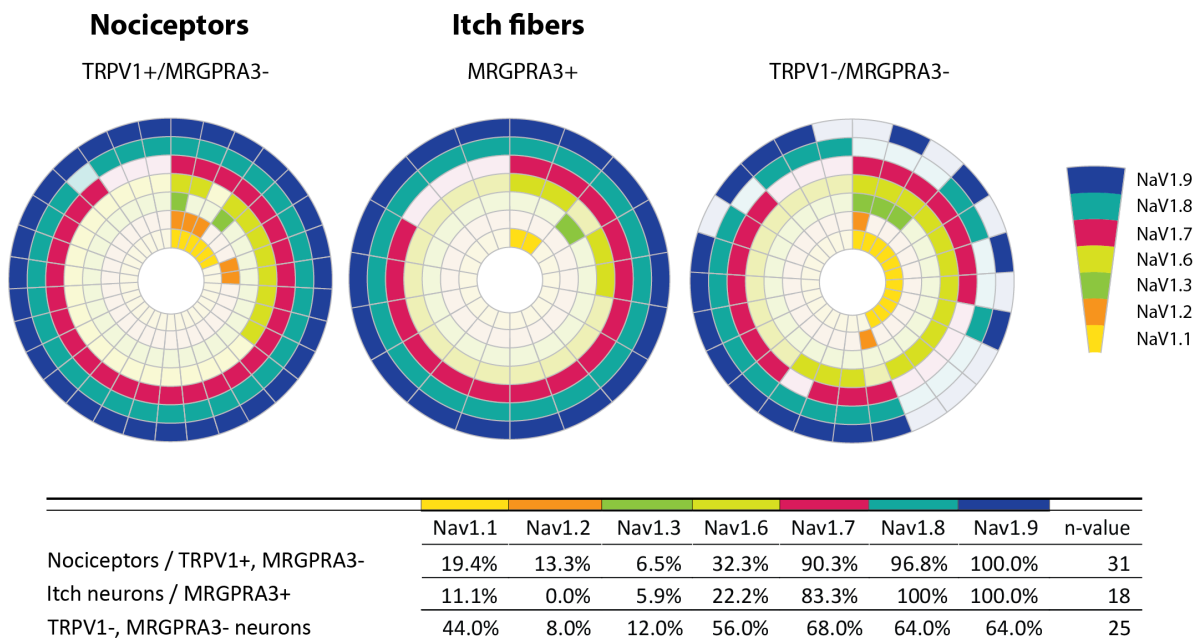


Figure 5

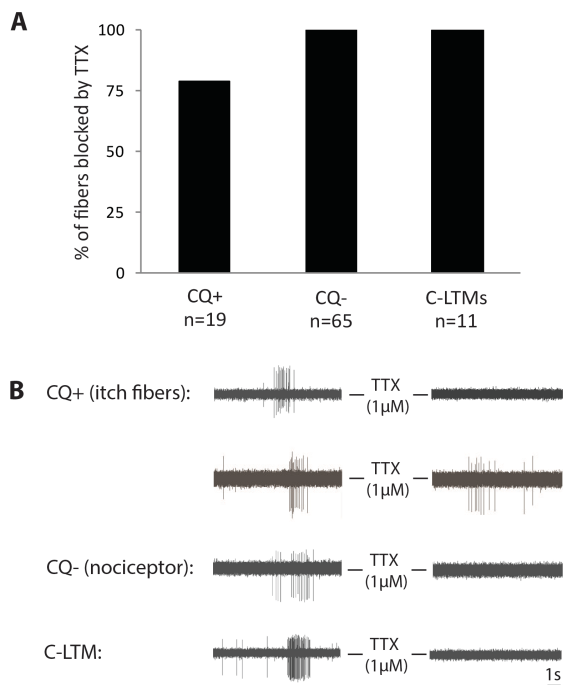


Figure 6

